3 RESULTS

3.1 Generation of conditional *Met* mutant mice

Met is a receptor tyrosine kinase that contains, like other nucleotide binding proteins, a Rothman motif (GXGXXG) in its cytoplasmic domain. This motif is essential for ATP binding and for the enzymatic activity of the receptor. Since *Met* knockout mice are not viable, I aimed to inactivate Met in a tissue specific manner. Therefore, I designed a targeting strategy that intended to mutate this ATP binding site conditionally (Fig. 3A). To achieve this, a targeting vector was constructed in which exon 15, which encodes the ATP binding site, was flanked by *lox*P sites. Upon expression of cre recombinase, the exon is deleted and a non-functional Met protein is produced from the mutant allele. The *lox*P sites should not interfere with the function of the 'floxed' gene and therefore the *lox*P sites were inserted in intron sequences that are not highly conserved among species. A backbone for constructing the targeting vector, the PTV-0-floxed neo vector was used. A 7.5kb genomic EcoRV-StuI fragment of the *Met* genomic locus including exon 15 was introduced into PTV-0-floxed neo vector, as a 5' homologous sequence. The short homologous arm was a 2kb Stu I /EcoR I fragment of genomic Met DNA. In addition, the targeting vector contained a positive selection marker, the neomycin resistance gene, and 0.7kb downstream of exon 15, which was also surrounded by *lox*P sites and could therefore be removed by recombination. The third *lox*P site was inserted into a Pac I restriction site, 0.6kb upstream of exon 15. The correct orientation of *lox*P sites was confirmed by sequencing and by *cre*-mediated recombination of the 'floxed' sequences *in vitro*.

The targeting vector was linearized at the 3' end of the short homology arm using Nhe I site and was then electroporated into E14.1/129 Ola ES cells (Thomas and Capecchi, 1987; Mansour et al., 1988). Two days after electroporation ES were selected with antibiotic G418 (Geneticin) for the presence of the *neomycin* resistance gene. A total of 800 colonies were picked and expanded; one aliquot of each clone was then frozen for storage, and another was used for the isolation of genomic DNA. Southern hybridization was used to detect homologous recombination events, and the presence of a single insertion event was verified. For this, external and internal probes derived from the *Met* locus as well as a specific probe for the *neomycin* resistance cassette, were used.

Among 500 screened ES clones, 16 had correctly inserted the vector by homologous recombination and contained thus the $Met^{flox}neo^{flox}$ allele, i.e. the recombination efficiency was 3.2%. The *neomycin resistance* gene can interfere with the expression of a 'floxed' allele, compromising its wild-type activity even in the absence of Cre-recombinase. Therefore, transient expression of Cre-recombinase was subsequently used to remove the *neo*-cassette in cells derived from two independent ES colonies (cf. Kuhn and Torres, 2002). The removal of the *neo*-cassette was controlled by Southern blot analysis of genomic ES cell DNA (Fig. 3B). Among 500-screened ES clones, 5 clones were identified that retained an intact 'floxed' exon 15 but had the *neomycin* resistance gene deleted. The 'floxed' *Met* allele will be referred to as the Met^{flox} allele in this work.

Two independent Met^{flox} +/- ES cell clones were injected into C57BL/6 blastocysts and transferred into foster mothers. From such blastocysts, chimeric mice developed, which have a spotty fur color. The ES cells used derive from the 129/Ola mouse strain that is characterized by an agouti (yellow) fur color, whereas the blastocysts derive from C57BL/6 mice that display black fur. The chimera contains cells from 129/Ola and from C57BL/6, and can be identified by a spotty yellow and black fur. The ES cells used here derive from a male animal, and chimeric females obtained from the injections have therefore usually a small ES cell contribution, and are often infertile. Therefore, five chimeric males from each ES clone were chosen and backcrossed to C57BL/6 females. If ES cells contribute to the germ line, the chimera can transmit the genetic information, also the mutant allele, to their offspring. This can be judged from the coat color of the offspring that is brown in animals that carry both, the agouti allele from the ES cells and the black allele of the C57BL/6 females. Brown offspring was identified, and germ line transmission of the Met^{flox} allele was analyzed by Southern blot analysis (Fig. 3C).

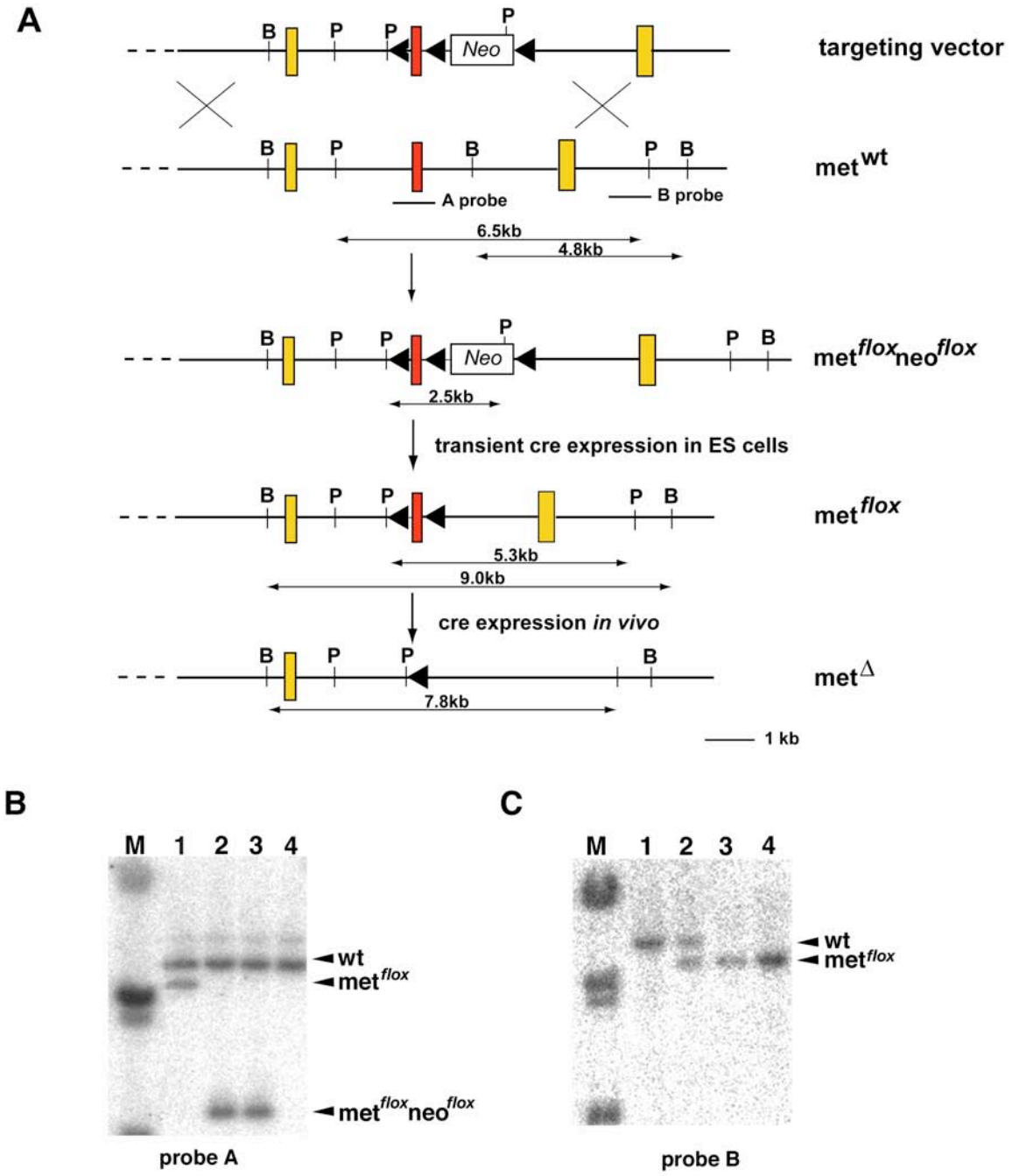

Figure 3. Generation of conditional *Met* mutant mice. (**A**) Schematic representation of targeting strategy employed to generate the Met^{flox} allele. Exon 15 of *Met*, encoding the ATP-binding site is presented as a red box. The yellow boxes indicate exons 14 and 16. The *lox*P sites (shown as arrowheads) flank the exon 15 and *neomycin* resistance gene (*Neo*). BamHI (=B) and PstI (=P) restriction site are indicated. The probes used for Southern blot analysis, as well as the predicted sizes of DNA fragments obtained after PstI and BamHI digestion, are shown. (**B**) After transient cre expression, ES cells were selected for the loss of the *Neo* cassette. Southern blot analysis of PstI-digested genomic DNA from Met^{flox}/+ ES cells (lane 1), $Met^{flox}neo^{flox}$/+ ES cells (lanes 2 and 3) and wild-type ES cells (lane 4). M, DNA size standard. (**C**) Southern blot analysis of PstI-digested genomic DNA from wild-type (lane 1), Met^{flox}/+ (lane 2) and Met^{flox}/ Met^{flox} (lanes 3 and 4) mice.

Heterozygous mice (F1) were then crossed to obtain homozygous *Met*^{flox} mice. In addition, the heterozygous animals were crossed with a strain that carries the Deleter-Cre (Schwenk et al., 1995), i.e. a *cre* transgene that is expressed early in development in all cells. Upon expression of cre recombinase, the exon 15 is deleted and a non-functional Met protein is produced from the mutant allele. This results in the generation of an animal that carries the *Met*$^{\Delta}$ allele in all cells of the body. *Met*^{flox}/*Met*^{flox} or *Met*$^{\Delta}$/+ mice were born with normal Mendelian frequencies, have a normal life span and did not show any overt abnormalities when compared to wild type mice. This indicates that the inserted *lox*P site in the *Met* locus does not interfere with Met function *in vivo*. Crosses of *Met*$^{\Delta}$/+ mice produced no live *Met*$^{\Delta}$/*Met*$^{\Delta}$ offspring. Further analysis of *Met*$^{\Delta}$ homozygous mice showed that they die during gestation and display the same phenotype as *Met-/-* or *HGF/SF-/-* mutants i.e. defective placenta and liver development as well as the absence of muscles derived from migrating muscle precursors (Bladt et al., 1995; Schmidt et al., 1995). This shows that the 'floxed' met allele can be recombined *in vivo* and that the resulting mutant allele corresponds to a functional null mutation.

3.2 Elimination of Met function in an adult liver

HGF/SF/Met signaling plays an important role for the growth of the liver during fetal development (Bladt et al., 1995; Schmidt et al., 1995). To analyze the function of Met in the adult liver i.e. after the completion of organ growth, I used the inducible *Mx-cre* allele to introduce a mutation of *Met* into liver cells (Kuhn et al., 1995). The *Mx* gene is a part of anti-viral defense and is activated in the presence of interferon. Furthermore, synthetic double stranded RNA (pIpC) is recognized as a viral agent and induces high levels of interferon. In the transgenic animal, the expression of cre is controlled by the *Mx* promoter, and can therefore be induced by interferon or by pIpC. The conditional *Met* mutant mice which I used for this study carried in addition to *Met*^{flox} and *Mx-cre* alleles, a *Met*^{null} allele; this ensured that only a single allele had to be recombined to obtain a complete ablation of *Met* function in the liver. Controls animals were heterozygous for the *Met*^{flox}/+ and also carried the *Mx-cre* allele. Both conditional *Met* mutant and control mice, were injected intraperitoneally with 300mg of pIpC, usually at an age of eight weeks. The injections of pIpC were repeated three times at intervals of two days. Two days after the last injection, recombination of the *Met*^{flox} allele was

almost complete in the liver as assessed by Southern blot analysis (Fig. 4A). Deletion of 'floxed' exon 15 does not result in a frame shift and therefore the Met transcript can be still detected. To verify that there is no functional Met protein present, auto-kinase assays were performed. No phosphorylated Met protein was detected in the extracts from livers of several conditional *Met* mutant mice (Fig. 4B).

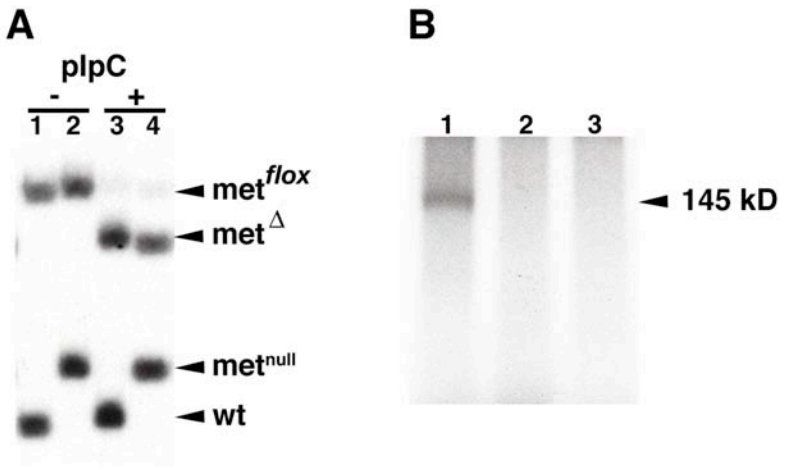

Figure 4. Ablation of Met in adult liver. (**A**) Southern blot analysis of PstI-digested genomic DNA isolated from the liver of *Mx-cre*; *Met*^{flox}/+ (lanes 1 and 3) and *Mx-cre*; *Metflox*/- (lanes 2 and 4) mice before (lanes 1 and 2) and after (lanes 3 and 4) pIpC injections. (**B**) Autophosphorylation assay of Met protein precipitated from liver extracts from *Mx-cre*; *Met*^{flox}/+ (lane 1) and *Mx-cre*; *Met*^{flox}/- animals 2 days after pIpC treatment (lane 2 and 3).

3.3 Met function in the normal liver

Conditional *Met* mutant mice were fertile, had a normal life span and showed no overt abnormalities. Histological analysis of livers three weeks after recombination did not reveal any differences in cellular architecture in conditional *Met* mutant mice when compared to controls (Fig. 3A and B). The liver plays an important role in lipid metabolism and disturbances in fatty acids synthesis or transport often lead to lipid accumulations, which can be detected by lipid-specific dyes like Oil Red O. In humans, an excessive accumulation of fat in hepatocytes is known as hepatic steatosis (Braunwald E. et al., 1998). Lipid accumulation was not observed in the liver three weeks after *Mx*-induced *Met* mutation (Fig. 5A and B). Another common pathological

condition in the liver is fibrosis, i.e. a replacement of hepatocytes by fibroblasts. Fibrosis is often associated with chronic liver disease and is a sign of liver injury and/or inflammation. Fibrosis is characterized by the accumulation of extracellular matrix proteins, mainly collagen types I and III. Masson´s trichrome staining can be used to monitor the increase in collagen content. However, Masson´s trichrome staining on liver sections did not demonstrate fibrosis in mice three weeks after the introduction of the *Met* mutation (data not shown). Thus, loss of Met does not cause steatosis or fibrosis within the first three weeks after the introduction of the mutation.

In contrast, six months after recombination, the liver histology of conditional *Met* mutant mice was abnormal. At this time point, small vesicles were observed by hematoxylin and eosin staining as well as by electron microscopy in the hepatocytes (Fig. 5 C, D and data not shown). These vesicles appeared in characteristic patterns. They accumulated mainly around the central vein and were rare in the peri-portal parts of liver lobules (Fig. 5D). These vesicles stained with Oil Red O, indicating that they were filled with fat (Fig. 5 E and F). Steatosis is associated with different conditions in humans, for instance with obesity, diabetes mellitus, high blood triglycerides and alcohol abuse (Braunwald et al., 1998). Overall, the accumulation of lipids is the most common response to liver stress. In the macrovesicular type of steatosis, large fat-filled droplets displace the nucleus to the periphery of the hepatocyte, as in an adipocyte. On the contrary, in conditional *Met* mutant mice the lipid droplets were small, and nuclei were located centrally in the hepatocytes (Fig. 7B and F). These features are characteristic of microvesicular steatosis. Together, these data indicate that the long-term loss of the Met tyrosine kinase receptor causes stress and impairs liver homeostasis.

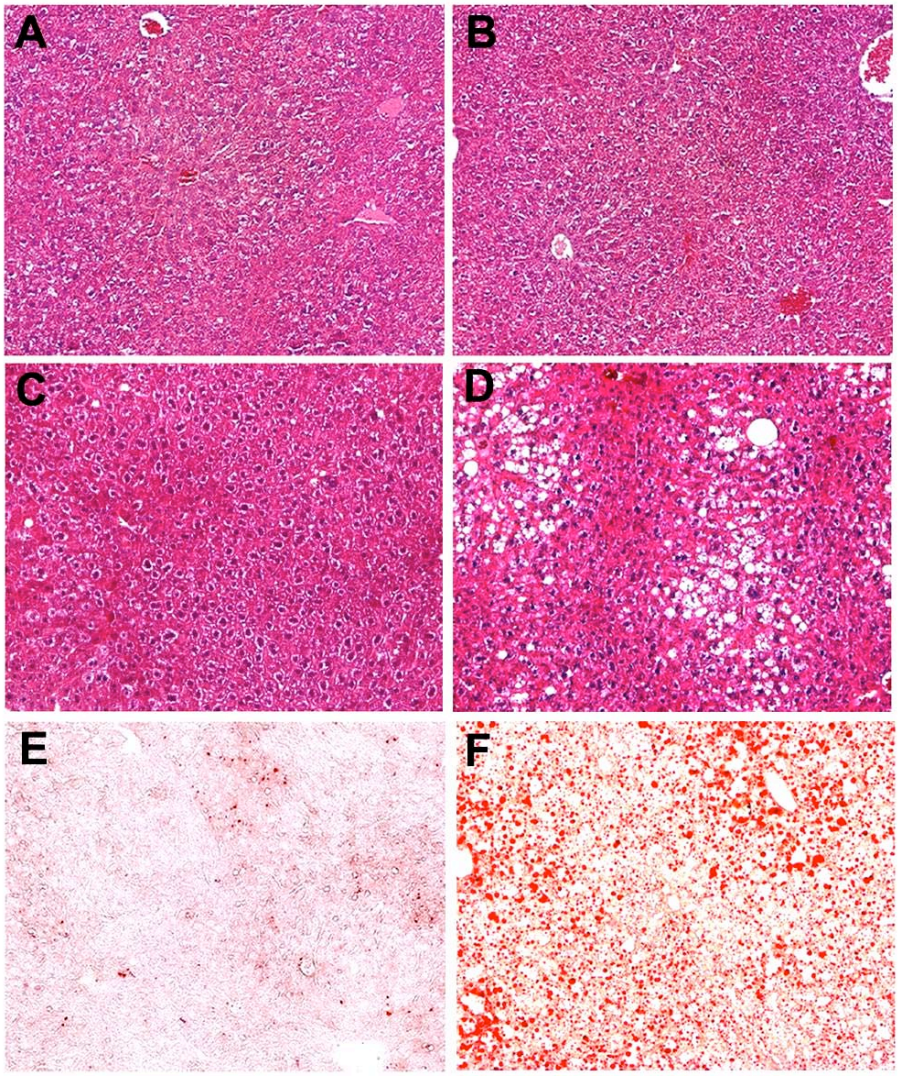

Figure 5. Histology of the liver in *Met*-deficient mice. Liver sections of control (**A**, **C**) and conditional *Met* mutant mice (**B**, **D**) stained with hematoxylin eosin three weeks (**A**, **B**) and 6 months (**C**, **D**) after the ablation of Met. Larger vesicles are observed in the old (**D**), but not in young conditional *Met* mutant mice (**C**). Neutral lipids are visualized as red droplets by Oil Red O staining of liver sections in control (**E**) and conditional *Met* mutant mice (**F**). Magnification x10 (A, B, E, F); x 20 (C, D).

3.4 Met is essential for liver regeneration

To analyze Met function in a stressed liver, I performed liver regeneration studies. The liver was injured by surgical excision of the median and left lobes, which comprise together a major portion of the liver, i.e. 65-70% of hepatic tissue. This model of liver injury is known as partial hepatectomy. For these partial hepatectomy experiments, only males at an age of 10-14 weeks were used, to exclude differences caused by the sex of

the animals. Furthermore, the surgery was always performed eight days after *Mx-cre* induction of the *Met* mutation. This allowed recuperation after the interferon responses, and ensured loss of the Met protein by turnover.

In the first set of experiments, partial hepatectomy was carried out as was described for rats (Anderson, 1931). Briefly, the skin and underlying muscle layer were cut transversally below the rib cage. Then the lateral and median lobes were ligated together and excised. All operated mice recovered from surgery shock, and I observed no difference between control and mutant mice during the first post-operative hours. However, 24 to 96 hours after partial hepatectomy, conditional *Met* mutant mice displayed weakness, lethargy and tremor, which were not noted in control animals. An increased mortality was observed in conditional *Met* mutant mice, and 95% of the operated animals (n=14) died within 2-3 days after partial hepatectomy. During the first three days after surgery, no liver growth was observed as assessed by BrdU incorporation in these conditional *Met* mutant mice. In contrast, all control animals (n=8) survived and regenerated their liver.

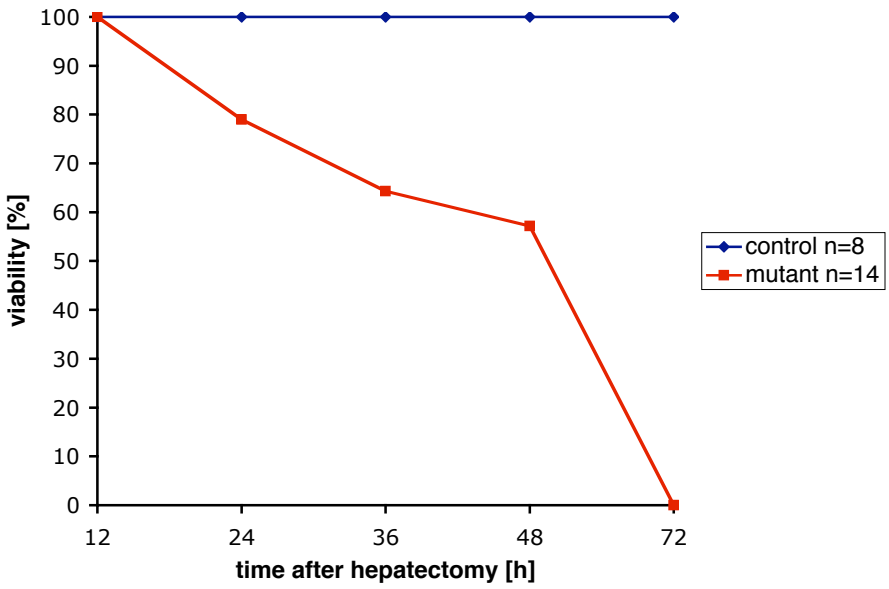

Figure 6. The survival of conditional *Met* mutant mice after the first set of partial hepatectomy experiments.

It has been previously observed that liver regeneration can be severely impaired in mutant mice, and that such impairment does also depend on the mode of surgery (Wüstefeld et al., 2003 and Cressman et al., 1996). I therefore changed the surgery method to one reported to be less stressful. A lower concentration of ketamine was used for anesthesia, and the abdominal cavity was opened by a longitudinal incision to minimize bleeding of the wound. Furthermore, each lobe was ligated and removed separately, and care was taken to avoid gall bladder damage. Under such conditions, all controls and 85% of conditional *Met* mutant mice survived. I therefore used this procedure to analyze Met functions during liver regeneration in all further experiments.

Two days after partial hepatectomy, the histology of the liver of conditional *Met* mutant and control mice was indistinguishable (data not shown). In all cases I observed lipid-filled vesicles (data not shown). Shortly after partial hepatectomy, the livers are stressed due to increased metabolic demands. Within the next days, when regeneration occurs, the livers of control mice recover and lipid droplets disappear. However, steatosis was pronounced during the regeneration process in conditional *Met* mutant mice (Fig. 7A-D), indicating that the recovery process was impaired.

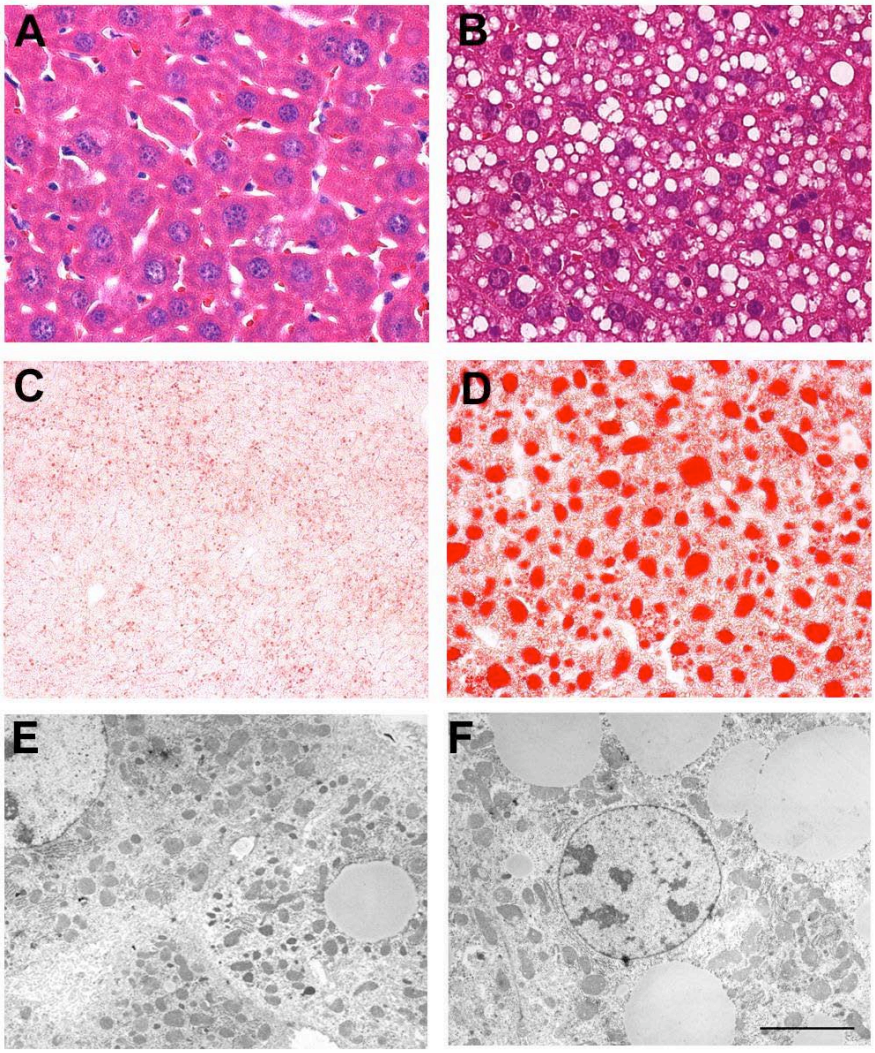

Figure 7. Liver histology five days after partial hepatectomy in mice that carry *Mx*-induced mutation of *Met*. Liver sections of control (**A**) and conditional *Met* mutant mice (**B**) five days after partial hepatectomy stained with hematoxylin-eosin. Oil Red O staining of liver sections of control (**C**) and conditional *Met* mutant mice (**D**). Lipid-filled vesicles are rarely observed in control animals (**C**) but are present at high numbers in regenerating livers of *Met* mutant mice (**D**). (**E, F**) Electron microscopy image of control (**E**) and *Met*-deficient liver (**F**) five days after partial hepatectomy.

Liver weight is precisely regulated during development and regeneration, to optimize its activity for the metabolic requirements of the animal. The critical determinant is the ratio between body and liver weight, which is constant between different individuals of a species. Before liver injury, the liver-to-body weight ratios were similar in the adult control and conditional *Met* mutant mice (Fig. 8). However, five to seven days after partial hepatectomy, the liver-to-body weight ratio of conditional *Met* mutant mice was

still below that observed for control animals (Fig. 8).

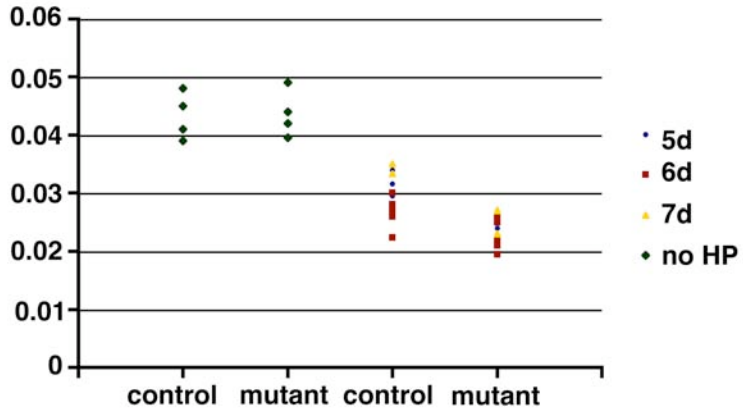

Figure 8. Liver size in conditional *Met* mutant mice several days after partial hepatectomy. Ratio of liver-to-body-weight in individual control and conditional *Met* mutant mice before surgery (green squares) and 5-7 days after partial hepatectomy.

I therefore analyzed proliferation and apoptosis of hepatocytes in the regenerating liver. To assess proliferation, I injected the thymidine analogue BrdU at different time points after partial hepatectomy; BrdU is incorporated into newly synthesized DNA and can be detected by immunohistochemistry. I analyzed nuclei that had incorporated the nucleotide one hour after BrdU injection. The first increase in the number of BrdU-positive nuclei can be observed 24 h after partial hepatectomy in the liver of control mice. 40 h after the operation, this increases further and reaches a peak 48 h after surgery. Five days after partial hepatectomy, hepatocyte replication has ceased (Fig. 9A and B). In conditional *Met* mutant mice, the proliferation of hepatocytes appeared in the same temporal manner, and peaked 48 h after partial hepatectomy. However, hepatocyte replication was lower during the entire replication phase, and peak number of BrdU positive nuclei was 60% reduced in *Met* mutant compared to control mice (Fig. 9A and B). This deficit in hepatocyte proliferation was not compensated at later time points and no BrdU incorporation was observed 5 days after surgery (Fig. 9A and B). Proliferation was also assessed by immunohistochemistry for Ki67, a nuclear protein expressed only by proliferating cells during the transition from the G1 to the M phase (Gerlach et al., 1997). The number of Ki67-positive nuclei in the liver was also

significantly lower in the conditional mutant mice (Fig. 9B and data not shown). Thus, proliferation of hepatocytes in the regenerating liver was impaired in conditional *Met* mutants.

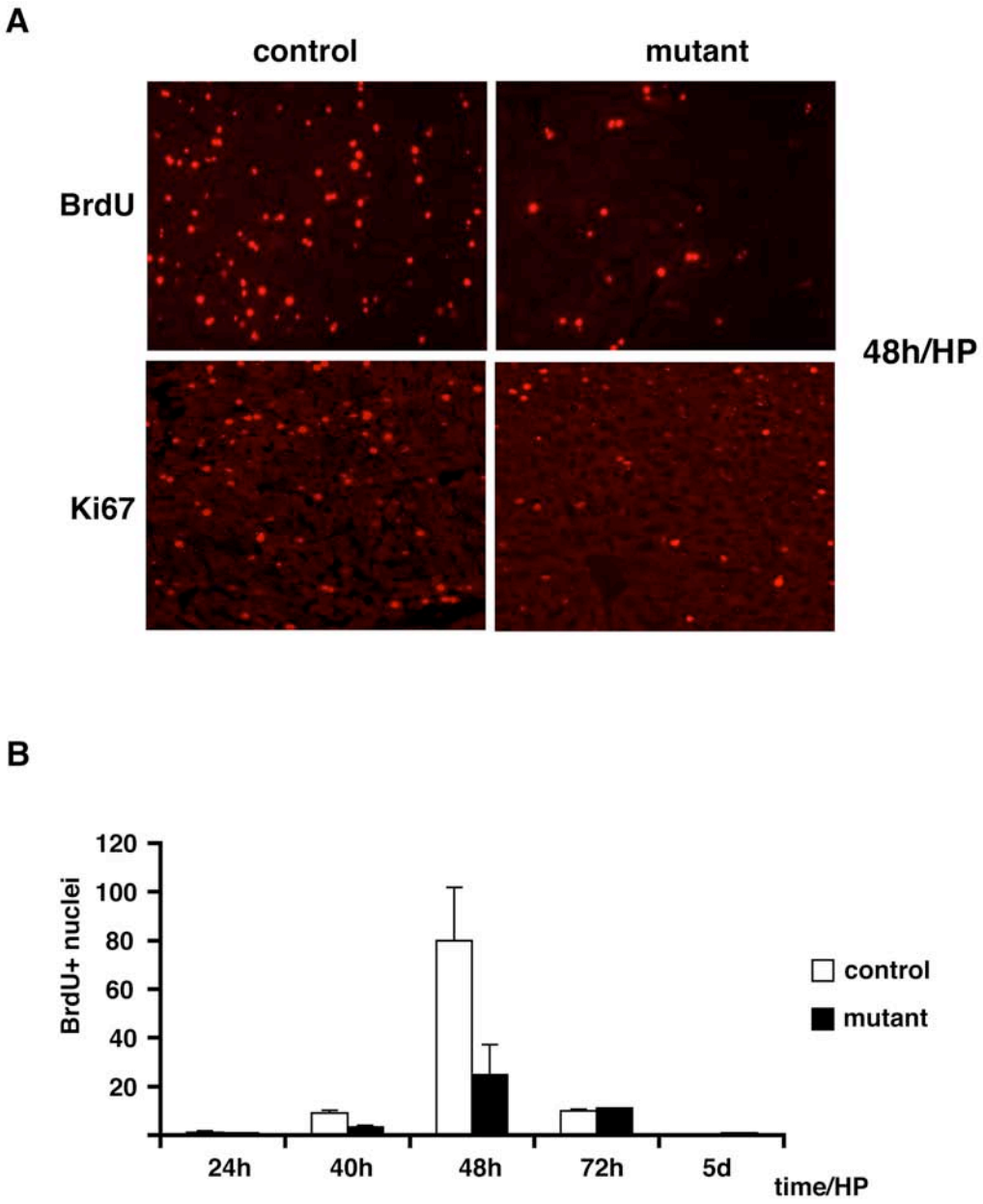

Figure 9. Decreased hepatocyte proliferation after partial hepatectomy in the absence of Met. (**A**) Immunohistochemistry of BrdU and Ki67 48h after partial hepatectomy in control and conditional *Met* mutant mice. Magnification 20x. (**B**) Quantification of BrdU-positive hepatocytes in control (white bars) and conditional *Met* mutant mice (black bars) at different time points after partial hepatectomy.

The inappropriate liver-to-body weight ratio might be also caused by an increased cell death. In addition, Met signaling promotes not only cell proliferation but prevents also programmed cell death (Wang et al., 2002a). During apoptosis, intracellular proteins are cleaved by proteases, for instance by caspase-3, carboxy-terminal of an aspartate residue. Caspases are first synthesized as pro-enzymes and their activation by cleavage serves as an early marker of apoptosis (Nicholson et al., 1995). A quantitative analysis of cleaved caspase-3 by Western blotting did not demonstrate a significant increase in the apoptosis of *Met*-deficient livers. Another characteristic event during apoptosis is the degradation of DNA, which can be detected by terminal deoxynucleotidyltransferase-mediated dUTP nick end labeling (TUNEL-assay) (Burgoyne et al., 1974). Apoptosis rates, as assessed by TUNEL-staining, were similar in control and conditional *Met* mutant mice (Fig. 10 and data not shown). This indicates that the impaired restoration of the liver mass was not caused by an increase in cell death.

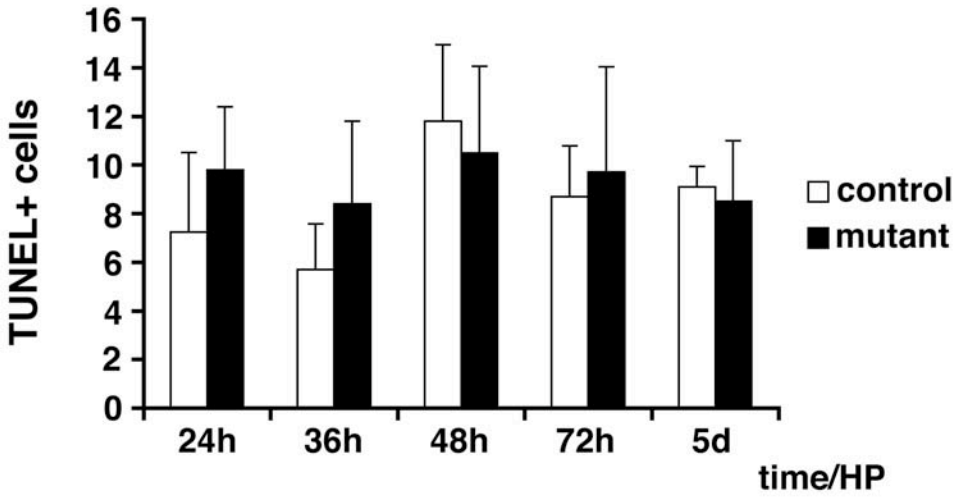

Figure 10. Apoptosis in the regenerating livers of conditional *Met* mutant mice. Quantification of TUNEL positive nuclei (per 30 microscopic fields) in control (white bars) and conditional *Met* mutant mice (black bars) at indicated time points after partial hepatectomy.

3.4.1 Exit from quiescence in the *Met*-deficient regenerating livers

Hepatocytes do not proliferate immediately after liver injury, because they are quiescent and have to gain replicative competence, i.e. they exit G0. This exit from G0 occurs synchronously during a first phase of liver regeneration, the priming phase. Expression or activation of immediate early genes, like c-fos and c-jun, is used to monitor the priming phase during liver regeneration (Behrens et al., 2002; Cressman et al., 1996; Servillo et al., 1998). Western blot analysis demonstrated that expression of c-fos was similar in control and conditional *Met* mutant mice and reached a peaked at 6 h after partial hepatectomy (Fig. 11). The activation of c-jun requires the phosphorylation of c-jun mediated by c-jun N-terminal kinase (JNK) (Westwick et al., 1995; Whitmarsh and Davis, 1996). High levels of phospho-c-jun protein were observed at 6 h in control and *Met*-deficient regenerating livers. However, subtle changes in the activation of c-jun were noticeable. In the liver of control mice, low levels of phospho-c-jun were still observed 12 h after partial hepatectomy (Fig. 11).

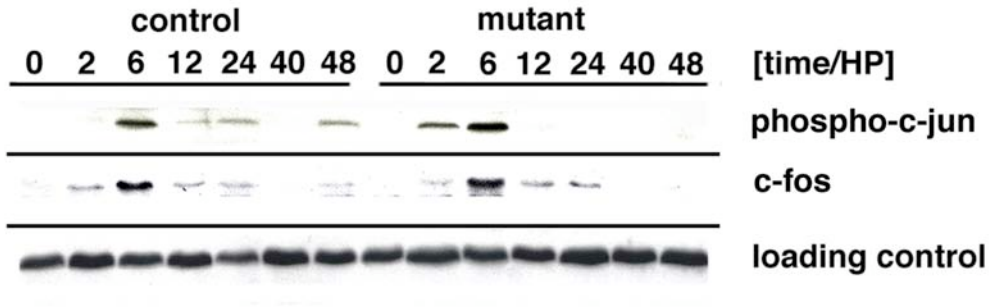

Figure11. Priming phase during liver regeneration in conditional *Met* mutant mice. Western blot analysis of phospho-c-jun and c-fos in control and conditional *Met* mutant mice at indicated time points after partial hepatectomy. As a loading control β-actin was analyzed.

The AP-1 transcription factor complex contains heterodimers and homodimers of c-fos, c-jun and related factors. The AP-1 controls the expression of cyclin D1, a gene expressed in G1 phase (Angel and Karin, 1991; van Dam et al., 1998). Cyclin D is the first cyclin that appears during cell cycle, and its accumulation is necessary for G1

progression (Albrecht and Hansen, 1999). In the regenerating liver of control mice, cyclin D1 accumulates over a long time period, is first observable at 12 h and reaches a peak at 40 h after partial hepatectomy. Expression of cyclin D1 is still observed 5 days after partial hepatectomy. In the livers of conditional *Met* mice, the peak of cyclin D1 expression appeared also at 40 h, but the levels were reduced. This deficit was not compensated at later time points (Fig. 12). This indicates that during liver regeneration, the transition from G0 to G1 is impaired in hepatocytes of conditional *Met* mutant mice.

3.4.2 Entry into S-phase during liver regeneration in conditional *Met* mutant mice

The next cyclin that is induced during cell cycle progression is cyclin E, which participates in regulation of the S-phase entry. In the regenerating liver of control mice, cyclin E appears 24 h after surgery, and the high levels of cyclin E are still observed 5 days (Fig. 12). Cyclin E appeared in the same schedule in the *Met*-deficient livers, but the levels were lower than those observed in control animals (Fig. 12).

Cyclins D and E, together with their catalytic partners, the cdks, phosphorylate pRb on several serine and threonine residues. This modification of pRb is a critical step of entry into S-phase: E2F is bound to pRb and is released and upon pRb phosphorylation (reviewed in : Harbour and Dean, 2000b; Weinberg, 1995). Free E2F activate then the expression of E2F-responsive genes. In the liver of control mice, the level of phospho-pRb peaks 48 h after surgery, which coincides with S-phase entry (Fig. 12). In the regenerating liver of *Met* mutant mice, high levels of phospho-pRb were observed at 48 h, but persisted longer and were still observable 5 days after partial hepatectomy (Fig. 12).

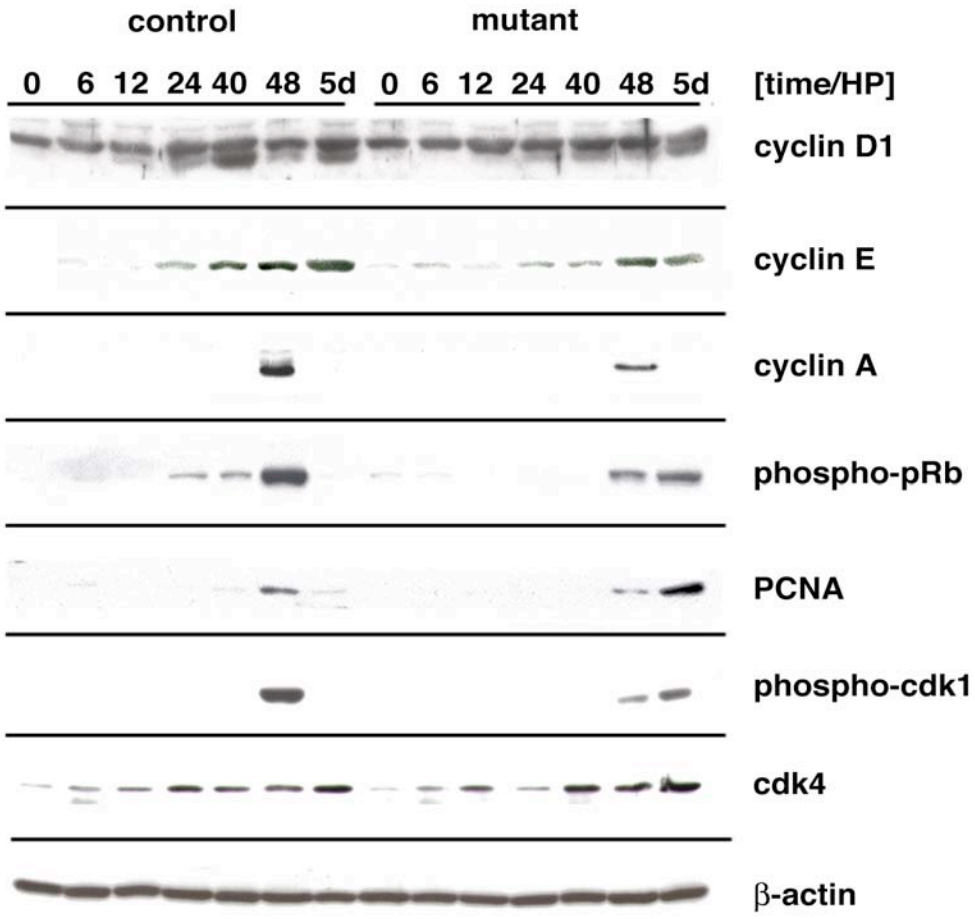

Figure 12. Exit from quiescence and cell cycle progression in conditional *Met* mutant mice. Western blot analysis of cyclin D1, cyclin E, cyclin A, phospho-pRb, PCNA, phospho-cdk1 and cdk4 in control and conditional *Met* mutant mice at indicated time points after partial hepatectomy. β-actin was analyzed as loading control for each separate blot. Note that in the first line the lower band corresponds to 36kDa cyclin D1.

Free E2Fs control transcription of fundamental regulatory genes that control S-phase entry, including PCNA, cyclin A, cdk1 and cdk4 (Trimarchi and Lees, 2002). PCNA functions as a co-factor for DNA polymerase delta during S-phase and DNA repair (Kurki et al., 1988). High levels of PCNA appear 48 h after partial hepatectomy in control and mutant mice (Fig. 12). However, even higher levels of PCNA were observed 5 days after surgery in the livers of *Met*-deficient mice (Fig.12). Cyclin A acts mainly in the S-phase of cell cycle, but it is also required for progression through G2, since mutation of cyclin A causes cells to arrest in G2. The peak levels of cyclin A coincide thus with the peak of BrdU incorporation. After cells enter S-phase, cyclin A is rapidly degraded by ubiquitin-mediated proteolysis (for recent review see Murray,

2004). Thus, cyclin A protein is not longer detectable by Western blot analysis 5 days after partial hepatectomy (Fig. 12). Expression of cyclin A appeared on schedule in conditional *Met* mutant mice, but at reduced levels (Fig. 12). Another molecule that is typically found during S-phase is phosphorylated cdk1 (Gautier et al., 1988). The modification in cdk1 at Thr14/Tyr15 is carried out by the Wee1 and Myt1 kinases and inactivates the cdk1-cyclin B complex. Termination of DNA synthesis is brought by cdc25 that dephosphorylates and thereby activates the cdk1-cyclin B complex, which is required for the subsequent G2/M transition (Juliano, 2003). Phosphorylation of cdk1 appears 48 h after surgery in control and mutant mice. Compared to control mice, phosphorylated cdk1 persisted longer in the regenerating liver of *Met* mutants and was still observable 5 days after surgery (Fig. 12). No difference was observed in expression of cdk4 (Fig. 12).

In conclusion, the expression or the activation of S-phase proteins correlates with DNA synthesis in the liver of control mice. However, in the mutant mice some of these S-phase proteins were present when hepatocyte proliferation had ceased. Thus, the control of S-phase entry does not occur correctly during liver regeneration in the conditional *Met* mutant mice.

3.4.3 Negative regulators of cell cycle progression during liver regeneration in conditional *Met* mutant mice

Not only proteins that signal S-phase entry, but also cell cycle inhibitors were activated in the liver of *Met* mutant mice five days after partial hepatectomy. The p21Cip1/Waf1 and p27/Kip1 proteins bind to and inhibit cyclin-cdk complexes in all phases of the cell cycle. These inhibitors can therefore induce cell cycle arrest in G1 or G2 respectively (Sherr and Roberts, 1999). Low levels of p21Cip1/Waf1 were observed 5 days after surgery in control mice, but p21Cip1/Waf1 was strongly up regulated in the liver of *Met* mutant mice (Fig. 13). Another member of the Cip/Kip family of cdks inhibitors, p27/Kip1 was expressed in the same manner in the regenerating livers of control and conditional *Met* mutant mice (data not shown).

The p21Cip1/Waf1 is a major target of the p53 pathway and activation of p53 often leads to an up-regulation in expression of p21Cip1/Waf1 (el-Deiry et al., 1993; Levine,

1997). Western blot analysis did show similar levels p53 levels in the livers of control and *Met* mutant mice (Fig. 13). Similarly, $p19^{ARF}$, which stabilizes p53 levels and therefore induces an arrest at the G1 and G2 checkpoints (Pomerantz et al., 1998) was expressed at similar levels in the control and *Met* mutant mice, indicating that p53 activity was not altered (Fig.13).

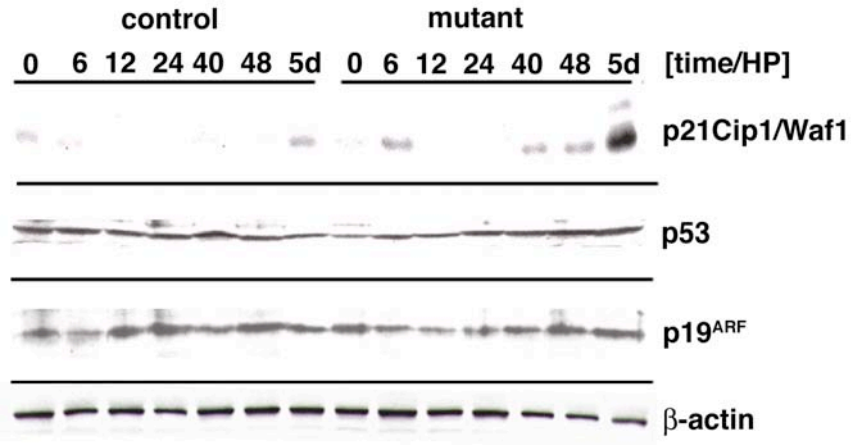

Figure 13. Cell cycle inhibitory signals in conditional *Met* mutant mice. Western blot analysis of p21Cip1/Waf1, p53, $p19^{ARF}$ in control and conditional *Met* mutant mice at indicated time points after partial hepatectomy. β-actin was analyzed as loading control for each separate blot.

3.4.4 Changes in the regulation of growth factors and cytokines in *Met* mutant mice after partial hepatectomy

Soon after partial hepatectomy, the levels of cytokines and growth factors like HGF/SF, IL-6 and TNF-α increase in the blood stream, which is one of the earliest observed responses to liver injury. Hepatocytes express the corresponding receptors and can therefore respond to these signals. These cytokines and growth factors are known to regulate the transcription of numerous growth-associated genes in cultured cells, and are thought to do this also in the regenerating liver (Diehl and Rai, 1996). I therefore compared the concentrations of circulating cytokines and growth factors in control and conditional *Met* mutant mice by ELISA assays.

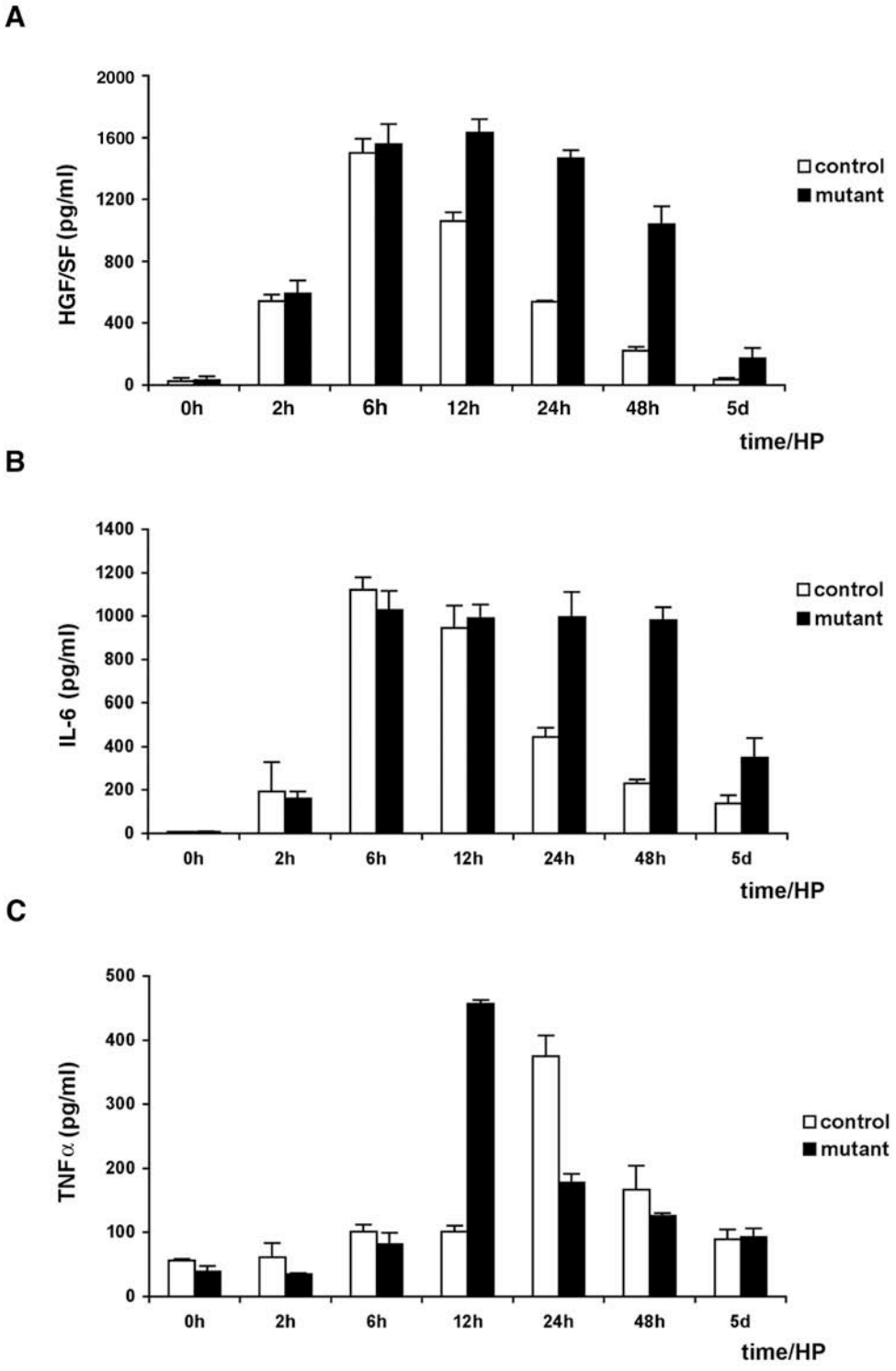

Figure 14. Circulating blood levels of HGF/SF, IL-6 and TNF-α in conditional *Met* mutant mice after partial hepatectomy. The concentrations of HGF/SF (**A**), IL-6 (**B**) and TNF-α (**C**) in the blood were analyzed by ELISA in control (white bars) and conditional *Met* mutant mice (black bars) at indicated time points after partial hepatectomy.

For this, blood was collected from the portal vein at various time points after partial hepatectomy. After blood clotting, the serum was collected. In the serum of control mice, levels of IL-6 and HGF/SF arise 2 h after surgery, and peak at 6 h (Fig. 14A and B). Subsequently, IL-6 and HGF/SF levels decline slowly, and reach concentrations that are comparable to the one observed before liver injury at 48 h (Fig. 14A and B). In conditional *Met* mutant mice, levels of IL-6 and HGF/SF increase in a similar manner and peaked 6-12 h after the operation. However, the up-regulated levels of IL-6 and HGF/SF were observed over a prolonged period, and elevated levels of HGF/SF and IL-6 were still observed 48 h after hepatectomy (Fig. 14A and B). Another cytokine, TNF-α appears at increased levels 24 h after surgery in control mice (Fig. 14C). In mutant animals, peak levels of TNF-α were observed 12 h earlier (Fig. 14C). The impaired liver regeneration in *Met*-deficient liver was thus accompanied by an aberrant regulation of cytokines and growth factors that circulate in the blood stream.

3.4.5 Signaling pathways activated during liver regeneration in control and conditional *Met* mutant mice.

Different pathways that control cell growth and survival are activated in the regenerating liver. Analysis of liver regeneration in conditional *Met* mutant mice creates an opportunity to identify the pathways activated in a Met-dependent manner.

The MAP kinase cascade is a key pathway used for the transmission of mitogenic signals in all eukaryotic organisms. All families of MAP kinases are activated during liver regeneration. The activation of MAP kinases depends on the phosphorylation of conserved threonine and tyrosine residues, mediated by MAP kinase kinase (MAPKK). Erk1 and Erk2 are MAP protein kinases regulated by extracellular signals and are effectors of Ras signaling; Erk1 and Erk2 have overlapping signaling capacities. High levels of phospho-Erk1/2 appear at 2 h and decline 40 h after surgery in the regenerating liver of control mice (Fig. 15). However, increased levels of phospho-Erk1/2 were not observed at any time in the *Met*-deficient livers (Fig. 15). Thus, the activation of Erk1/2 MAP kinases in the regenerating liver depends exclusively on Met signaling.

Another member of the MAP kinase family, p38, is mainly activated by inflammatory cytokines and by environmental stress and requires phosphorylation mediated by MEK3

and MEK6 kinases (Lee et al., 1994). I wanted to test if conditional *Met* mutant mice are subjected to extended stress or inflammation that might have an impact on liver regeneration. Phosphorylation of p38 kinase occurred in the same manner in the liver of control and *Met*-deficient mice (Fig. 15).

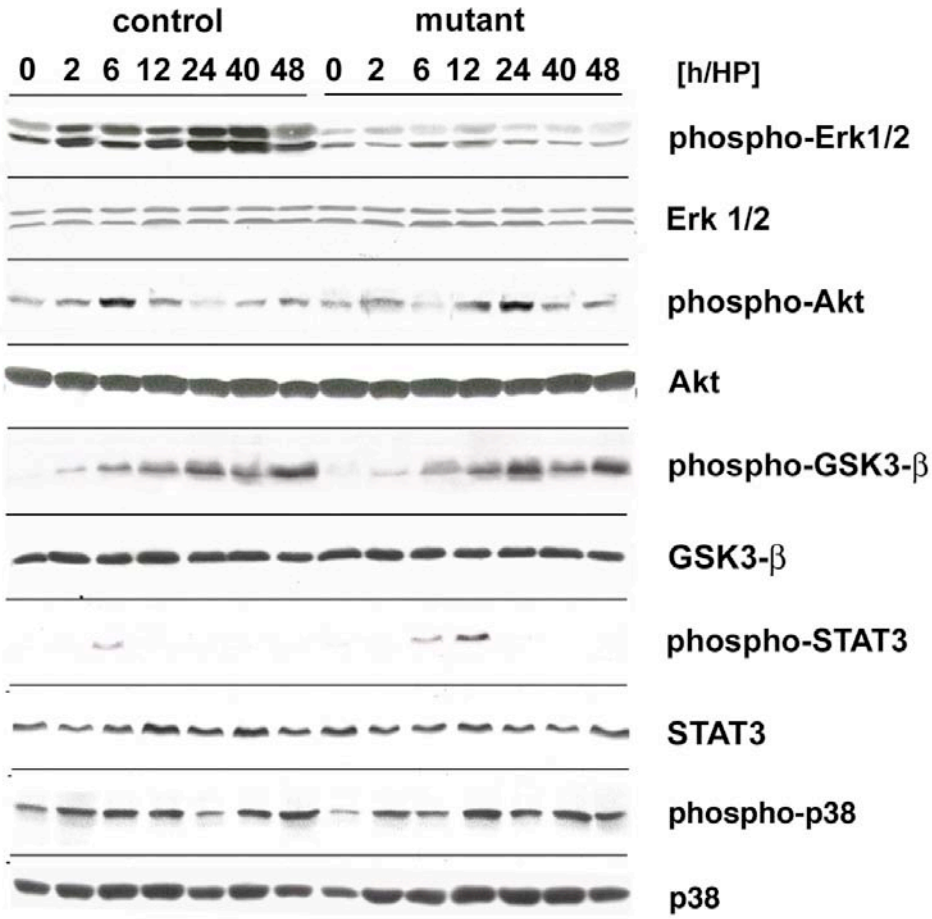

Figure 15. Signaling pathways activated in the regenerating liver of conditional *Met* mutant mice. Western blot analysis of phospho-Erk1/2, total Erk1/2 protein, phospho-Akt, total Akt protein, phospho-GSK3-β, total GSK3-β protein, phospho-STAT3, total STAT3 protein, phospho-p38 and total p38 protein in control and conditional *Met* mutant mice is presented at indicated time points after partial hepatectomy.

Another important mediator of cell growth and survival is the Akt kinase. Activation of Akt is controlled by PI3K, which in turn is activated by growth factors. Phospholipids generated by PI3K bind directly to the PH domain of Akt, which allows translocation of

cytosolic Akt to the plasma membrane. This brings Akt in close proximity to the regulatory kinases that can activate Akt. Akt phosphorylation occurs in two steps, firstly on Thr308, mediated by phosphoinositide-dependent protein kinase 1 (PDK1). Subsequently, Akt is phosphorylated on Ser473 by the Akt kinase itself or by PDK2 (Toker and Newton, 2000). Full activation of Akt requires phosphorylation on both sites, and was analyzed on Western blots using phospho-Ser473-Akt antibodies. In control mice, phosphorylation of Akt is observed 6 h after surgery (Fig. 15). In the *Met* mutant mice, the peak of Akt activation was observed at 24 h (Fig. 15).

To analyze whether delayed Akt activation has an impact on downstream signaling, a major target of Akt, glycogen synthase kinase 3 (GSK3-β), was analyzed. Akt phosphorylates GSK3-β on Ser9, which turns off the catalytic activity of GSK3-β and activates pathways that are normally repressed by GSK3-β (reviewed by Cohen and Frame, 2001). Phosphorylation of GSK3-β occurred on the same schedule and to the same extents in the livers of control and *Met* mutant mice (Fig. 15). Thus, the change in the activation of the Akt pathway does not affect the repression of GSK3-β, indicating that GSK3-β activity is altered by other kinases than Akt.

Gp130 is an essential subunit of the receptor complex for the IL-6 family of cytokines, which include leukemia inhibitory factor (LIF) and oncostatin M (OSM) (Hibi et al., 1990). Binding of IL-6 to gp130 leads to receptor homo- or heterodimerization with other gp130 related receptors, which results in the activation of Janus kinases (JAK) and, subsequently, in the recruitment and activation of STAT3 and other signal transducers. Activation of STAT3 requires its phosphorylation at a conserved tyrosine residue, which is mediated by JAK. The phosphorylated STAT3 dissociates then from gp130 and translocates to the nucleus (reviewed by (Hirano et al., 2000). Phosphorylation of the tyrosine residue 705 of STAT3 peaks at 6 h after partial hepatectomy in livers of control mice, which correlates with the peak of IL-6 concentration in the blood (Fig. 15). In conditional *Met* mutant mice, phosphorylation of STAT3 persisted and was still elevated 12 h after surgery, which is in accordance with the prolonged up-regulation of IL-6 (Fig. 15).